that was mentioned in the Introduction and has been exploited by us[4] and others.[34]

Summary

This study adds further examples to the rapidly growing number of organometallic mixed-valence complexes.[2b,35] The combination of "hard" ligands which are commonly used with more "inorganic" metal fragments[12-15] and the weakly electrophilic organometallic fragments $[Cp(CO)_2Mn]^{0/+}$ [4,26] results in an unsatisfactory situation as concerns coordinative stability; we shall try to overcome this problem by using either more electrophilic metal fragments or even more basic bridging ligands. Nevertheless, it has been possible with some ligand systems to change from $Ru^{II}Ru^{III}$ ammine to organometallic $Mn^{I}Mn^{II}$ systems without affecting the position and shape of the IT transition but with having the valuable opportunity for convenient EPR studies of the spin distribution.[33b]

One reason to use small biochemically relevant O and N ligands in this study despite the preparative difficulties was to answer the question whether further spectroscopic knowledge can be gathered with regard to mixed-valence manganese species such as the ones observed during irradiation of photosynthetic O_2-evolving complexes in chloroplast membranes.[8] There are mixed-valence $Mn^{I}Mn^{II}$ complexes with one,[25c] two,[9] or three[7e] thiolate bridges, and other approaches have included the use of sulfur ligands to stabilize higher-valent manganese as mixed-valence species[7f] or in the presence of μ-imidazolate[7f,13g,h] or μ-OR ligands;[14e] however, EXAFS studies of enzymatic material have strongly suggested that the first coordination shell around the Mn centers contains only light donor atoms such as O or N and that the manganese atoms are in close contact, possibly bridged by O.[36] Although the photosynthetic processes do not involve manganese in the +I oxidation state or in organometallic form[8] and model systems involving higher valent Mn and oxo ligands[7c] are certainly more realistic (oxygen is *used* and not *produced* in our system), the application of the alkoxide/oxide analogy[37] may stimulate further investigation and speculation on the nature of the photosynthetically active manganese centers.[8i]

A final comment should be made on the relation between ^{55}Mn coupling constants and oxidation-state assignments. The isotropic values $a_{^{55}Mn}$ of organometallic low-spin Mn^{II} and $Mn^{I}Mn^{II}$ (doubled value) range from 5.4 mT (alkoxide-bridged dimers) to 6.1 mT (imidazolate-bridged dimer and monomer) and 6.4 mT (alkoxide-coordinated monomers) to 6.6 and 7.2 mT for thiolate- and methylene-bridged dimers,[7e,9,10] thus illustrating again[7d] the difficulty of determining metal oxidation states[8g] from EPR hyperfine values only.

Acknowledgment. This work has been supported by the Deutsche Forschungsgemeinschaft (DFG), Fonds der Chemischen Industrie, Flughafen Frankfurt/Main AG, and the Hermann Willkomm-Foundation. We wish to thank Dr. K. Pohl and Professor K. Wieghardt (Ruhr Universität Bochum) for absorption measurements in the near-IR region and Professor H. Taube (Stanford University) for communication of unpublished results.

---

(34) Lynch, M. W.; Hendrickson, D. N.; Fitzgerald, B. J.; Pierpoint, C. G. *J. Am. Chem. Soc.* **1984**, *106*, 2041.

(35) (a) Babonneau, F.; Henry, M.; King, R. B.; El Murr, N. *Inorg. Chem.* **1985**, *24*, 1946. (b) Casewit, C. J.; Rakowski DuBois, M. *Ibid.* **1986**, *25*, 74. (c) Scherer, O. J.; Schwalb, J.; Wolmershäuser, G.; Kaim, W.; Gross, R. *Angew. Chem.* **1986**, *98*, 349 *Angew. Chem., Int. Ed. Engl.* **1986**, *25*, 363.

(36) (a) Kirby, J. A.; Robertson, A. S.; Smith, J. P.; Thompson, A. C.; Cooper, S. R.; Klein, M. P. *J. Am. Chem. Soc.* **1981**, *103*, 5529. (b) Kirby, J. A.; Goodin, D. B.; Wydrzynski, T.; Robertson, A. S.; Klein, M. P. *Ibid.* **1981**, *103*, 5537.

(37) Chisholm, M. H. *J. Solid State Chem.* **1985**, *57*, 120.

Contribution from the Département de Chimie,
Université de Montréal, Montréal, Québec, Canada H3C 3J7

Preparation and Structural Studies of Methylmercury Compounds Containing Amino-Deprotonated Adenine

Jean-Pierre Charland and André L. Beauchamp*

Received April 30, 1986

Reaction of CH_3HgOH with adenine (HAd) in water–ethanol mixtures yielded 2:1 and 3:1 compounds. Substitution of the imidazole proton and one of the amino protons in $[(CH_3Hg)_2(Ad\text{-}H)]\cdot EtOH$ was deduced from the IR spectra. Crystals of $[(CH_3Hg)_3(Ad\text{-}2H)]\cdot{}^1/_2H_2O$ are monoclinic, $C2/c$, with $a = 20.809$ (7) Å, $b = 7.263$ (1) Å, $c = 18.788$ (1) Å, $\beta = 104.91$ (4)°, and $Z = 8$. The structure was refined on 1104 nonzero Mo Kα reflections to $R = 0.050$. The imidazole proton and both of the amino protons have been substituted by linearly coordinated CH_3Hg^+ groups in this compound. Reaction of CH_3HgOH and CH_3HgX ($X = NO_3^-$, ClO_4^-) led to isolation of compounds of the type $[(CH_3Hg)_4(Ad\text{-}2H)]X$. Crystals of $[(CH_3Hg)_4(Ad\text{-}2H)]NO_3$ are monoclinic, $P2_1/c$, with $a = 14.458$ (5) Å, $b = 7.478$ (1) Å, $c = 20.174$ (5) Å, $\beta = 126.34$ (2)°, and $Z = 4$. The structure was refined on 1502 nonzero Cu Kα reflections to $R = 0.053$. This compound contains NO_3^- anions and $[(CH_3Hg)_4(Ad\text{-}2H)]^+$ cations, in which three CH_3Hg^+ groups occupy the same sites as in the above compound, whereas the fourth CH_3Hg^+ group is bound to N3. The infrared spectra of these compounds and of their C8-deuteriated derivatives were compared with those of CH_3HgAd, and diagnostic regions were identified to characterize each type of bonding. The ^1H and ^{13}C NMR results are discussed.

Introduction

As part of our continuing research on the binding of the CH_3Hg^+ cation with DNA bases, a series of adenine complexes (Chart I) have been structurally characterized in this laboratory.[1-6] They invariably showed that metal complexation first occurred with N9 by substitution of the labile acidic H9 proton. Extra CH_3Hg^+ groups could be introduced into the ring without proton displacement. They were found to bind first to N7 and then to

---

(1) Prizant, L.; Olivier, M. J.; Rivest, R.; Beauchamp, A. L. *J. Am. Chem. Soc.* **1979**, *101*, 2765–2767.

(2) Beauchamp, A. L. *J. Cryst. Mol. Struct.* **1980**, *10*, 149–156.

(3) Hubert, J.; Beauchamp, A. L. *Acta Crystallogr., Sect. B: Struct. Crystallogr. Cryst. Chem.* **1980**, *B36*, 2613–2616.

(4) Hubert, J.; Beauchamp, A. L. *Can. J. Chem.* **1980**, *58*, 1439–1443.

(5) Prizant, L.; Olivier, M. J.; Rivest, R.; Beauchamp, A. L. *Acta Crystallogr., Sect. B: Struct. Crystallogr. Cryst. Chem.* **1982**, *B38*, 88–92.

(6) Prizant, L.; Olivier, M. J.; Rivest, R.; Beauchamp, A. L. *Can. J. Chem.* **1981**, *59*, 1311–1317.

0020-1669/86/1325-4870$01.50/0

Chart I

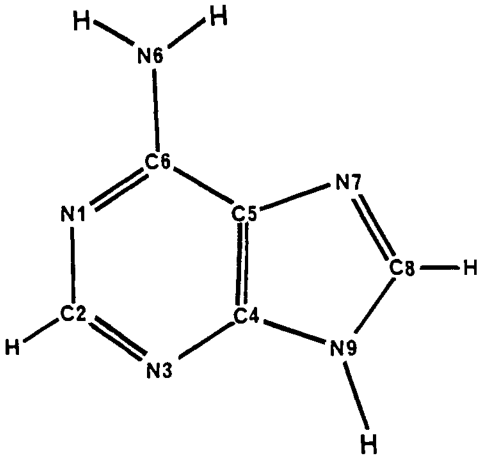

N3. Up to now, the CH_3Hg^+ ion has never been observed to bind to N1 in adenine. Reaction also takes place with the amino group. The amino lone pair is not normally available for metal complexation, as it is delocalized into the ring π system.[7] Nonetheless, substitution of one of the amino protons by metal ions does occur for the cytosine residue, examples having been reported for Pt,[8] Ru,[9] Ag,[10,11] and Hg[12-15] either in the solid state or in solution. In the case of adenine, a similar behavior is known only for Ag[15] and Hg.[1,13,14,16] In an earlier report,[1] it was shown that the CH_3Hg^+ ion smoothly displaced an amino hydrogen of 9-methyladenine (MAd)[17] under mild conditions. This prompted us to examine the possibility of displacing both amino hydrogens.

The present paper deals with a new series of CH_3Hg^+ complexes with adenine (HAd),[17] in which the metal-to-base ratio ranges from 2:1 to 4:1. Their infrared spectra were examined in detail to relate the site of complexation on adenine with characteristic spectral changes. The crystal structures of two of these compounds were determined by X-ray diffraction, whereas their behavior in solution was examined by means of ^1H and ^{13}C NMR. Some of these results have been briefly described.[18]

Experimental Section

Preparations. Adenine (Terochem) and CH_3HgOH (1 M aqueous solution, Alfa) were used without further purification. CH_3HgI (Alfa) was the starting material to prepare water solutions (~0.4 M) of CH_3HgNO_3 and CH_3HgClO_4 as described elsewhere.[12]

Preparations were usually run with 1 mmol (0.135 g) of adenine in suspension in warm ethanol. Suitable volumes of CH_3HgNO_3, CH_3HgClO_4, and/or CH_3HgOH solutions were added to obtain the required metal-to-ligand ratio. Even if adenine is practically insoluble in absolute ethanol, addition of the aqueous methylmercury reactants rapidly produced homogeneous solutions. Prolonged heating of the mixture proved unnecessary. CH_3HgOH, which acts as a base, was used when abstraction of an acidic proton was required. CH_3HgNO_3 and CH_3HgClO_4 supplied the CH_3Hg^+ cations for reactions without proton loss. The final mixtures were allowed to stand at room temperature until ~80% of the solvent had evaporated. The crystals were then collected and washed with ethanol and ether. Yields were >60%. When examined under the microscope, each of these crystalline samples was found to be morphologically uniform. This was considered as evidence for high purity. The crystals were stable in air, but they turned yellowish after standing in closed containers for extended periods of time. The compounds prepared are listed below, together with the quantities of methylmercury solutions reacted with 1 mmol of ligand. All analyses were carried out by Schwarzkopf Laboratories, Woodside, NY.

Table I. Crystallographic Data

	2	**3a**
formula	$C_8H_{11}Hg_3N_5\cdot{}^1/_2H_2O$	$C_9H_{14}Hg_4N_6O_3$
fw	788.0	1056.6
cryst syst	monoclinic	monoclinic
space group	$C2/c$	$P2_1/c$
a, Å	20.809 (7)	14.458 (5)
b, Å	7.263 (1)	7.478 (1)
c, Å	18.788 (1)	20.174 (5)
β, deg	104.91 (4)	126.34 (2)
V, Å^3	2743.9	1756.9
Z	8	4
D_c, g cm^{-3}	3.814	3.993
cryst dimens, mm^3	0.26 × 0.28 × 0.12	0.027 × 0.054 × 0.115
radiation (λ, Å)	Mo K$\bar{\alpha}$ (0.710 69)	Cu K$\bar{\alpha}$ (1.541 78)
octants measd	hkl, $hk\bar{l}$ ($h + k = 2n$)	hkl, $hk\bar{l}$
max 2θ	50.0	120.0
no. of indep reflcns	2406	2612
no. of nonzero reflcns	1104	1502
av std fluctuatns, %	2.9	1.7
abs coeff, cm^{-1}	334.6	661.6
transmissn range	0.023–0.072	0.058–0.271
R factor[a]	0.050	0.053
R_w factor[a]	0.053	0.058
goodness-of-fit ratio	1.56	1.58

[a] $R = \sum||F_o| - |F_c||/\sum|F_o|$; $R_w = (\sum w(|F_o| - |F_c|)^2/\sum w|F_o|^2)^{1/2}$.

$[(CH_3Hg)_2(Ad\text{-}H)]\cdot C_2H_2OH$ (1). CH_3HgOH (2 mmol) in a total volume of 20 mL of reaction mixture. Anal. Calcd for $C_9H_{15}Hg_2N_5O$: Hg, 65.7; C, 17.7; H, 2.5; N, 11.5. Found: Hg, 65.9; C, 17.7; H, 2.2; N, 11.7.

$[(CH_3Hg)_3(Ad\text{-}2H)]\cdot{}^1/_2H_2O$ (2). CH_3HgOH (3 mmol) in a total volume of 20 mL. Also obtained from 4 or 5 mmol of CH_3HgOH in 20 mL. Anal. Calcd for $C_{16}H_{24}Hg_6N_{10}O$: Hg, 76.4; C, 12.2; H, 1.5; N, 8.9. Found: Hg, 77.0; C, 12.1; H, 1.5; N, 8.9.

$[(CH_3Hg)_4(Ad\text{-}2H)]NO_3$ (3a). CH_3HgNO_3 (1 mmol) and CH_3HgOH (3 mmol) in a total volume of 30 mL. Anal. Calcd for $C_9H_{14}Hg_4N_6O_3$: Hg, 75.9. Found: Hg, 75.6. A crystal from the homogeneous sample was shown to have the indicated composition by X-ray diffraction (see below).

$[(CH_3Hg)_4(Ad\text{-}2H)]ClO_4$ (3b). CH_3HgClO_4 (1 mmol) and CH_3HgOH (3 mmol) in a total volume of 30 mL. Anal. Calcd for $C_9H_{14}ClHg_4N_5O_4$: Hg, 73.3; C, 9.9; H, 1.3; N, 6.4. Found: Hg, 73.6; C, 10.0; H, 1.4; N, 6.5.

$[(CH_3Hg)_3(Ad\text{-}H)]NO_3$ (4) was prepared as described earlier.[6]

Infrared Spectroscopy. The spectra (4000–400 cm^{-1}) were recorded as KBr pellets by using a Beckman IR 4250 spectrophotometer.

C8-deuteriated samples of compounds **1**–**3** were prepared for NMR[19] and infrared work (see below). The starting adenine was obtained by refluxing a saturated solution in D_2O (Merck, Sharp and Dohme Canada) for 2.5 h. The solid filtered from the cold solution was adenine-*6,6,8,9*-d_4, and deuteriation at C8 was found to be complete by ^1H NMR. The above reactions were repeated with this deuteriated adenine. Since the solvent was an ordinary H_2O–ethanol mixture, the N–H groups rehydrogenated, but the C8-bound deuterium was not exchanged, as it was checked by NMR.

NMR Measurements. Samples for ^1H NMR were made by dissolving 10–20 mg of material in 1.0 mL of Me_2SO-d_6 (Merck, Sharp & Dohme Canada or Cambridge Isotope Laboratory). Saturated solutions were used for the ^{13}C spectra. Me_4Si or occasionally the residual solvent signals (conversion factors are 2.500 ppm for ^1H and 39.40 ppm for ^{13}C) were used as internal references. The spectra were recorded with either

---

[7] Marzilli, L. G. *Prog. Inorg. Chem.* **1977**, *23*, 255–378.

[8] Faggiani, R.; Lippert, B.; Lock, C. J. L.; Speranzini, R. A. *J. Am. Chem. Soc.* **1981**, *103*, 1111–1120.

[9] Clarke, M. J. *J. Am. Chem. Soc.* **1978**, *100*, 5068–5075. Graves, B. J.; Hodgson, D. J. *J. Am. Chem. Soc.* **1979**, *101*, 5608–5612.

[10] Cini, R.; Colamarino, P.; Orioli, P. L. *Bioinorg. Chem.* **1977**, *7*, 345–349.

[11] Butzow, J. J.; Clark, P.; Tarien, E.; Eichhorn, G. L. *Biopolymers* **1968**, *5*, 283–296.

[12] Prizant, L.; Rivest, R.; Beauchamp, A. L. *Can. J. Chem.* **1981**, *59*, 2290–2297.

[13] Taylor, S. E.; Buncel, E.; Norris, A. R. *J. Inorg. Biochem.* **1981**, *15*, 131–141.

[14] Simpson, R. B. *J. Am. Chem. Soc.* **1964**, *86*, 2059–2065. Mansy, S.; Frick, J. P.; Tobias, R. S. *Biochim. Biophys. Acta* **1975**, *378*, 319–332.

[15] Gillen, K.; Jensen, R.; Davidson, N. *J. Am. Chem. Soc.* **1964**, *86*, 2792–2796.

[16] Eichhorn, G. L.; Clark, P. *J. Am. Chem. Soc.* **1963**, *85*, 4020–4024.

[17] The following symbols are used: HAd, neutral adenine; Ad$^-$, adenine monoanion having lost the imidazole proton; [Ad-H]$^{2-}$, adenine dianion having lost the imidazole and one amino proton; [Ad-2H]$^{3-}$, adenine trianion having lost the imidazole and both amino protons; MAd, neutral 9-methyladenine.

[18] Charland, J. P.; Simard, M.; Beauchamp, A. L. *Inorg. Chim. Acta* **1983**, *80*, L55–L56.

[19] St-Jacques, M.; Tan, P. V. M.; Charland, J. P.; Beauchamp, A. L. *J. Am. Chem. Soc.* **1985**, *107*, 8202–8211.

Table II. Refined Fractional Coordinates and Equivalent Temperature Factors

atom	x	y	z	U_{eq}
		$[(CH_3Hg)_3(Ad\text{-}2H)]\cdot{}^1/_2H_2O$ (**2**)		
Hg9	1265 (1)	4761 (2)	2466 (1)	49
Hg61	1911 (1)	−5298 (2)	4621 (1)	64
Hg62	3310 (1)	−3092 (2)	4097 (1)	61
N1	129 (2)	−205 (5)	402 (2)	70
N3	91 (1)	84 (4)	342 (2)	54
N6	235 (2)	−338 (4)	407 (2)	69
N7	256 (1)	19 (4)	325 (2)	52
N9	177 (1)	245 (4)	292 (1)	52
C2	87 (2)	−60 (6)	381 (2)	58
C4	152 (2)	95 (5)	329 (2)	48
C5	203 (2)	−30 (4)	351 (2)	35
C6	192 (2)	−198 (5)	387 (2)	53
C8	237 (2)	179 (6)	294 (2)	48
C9	74 (2)	708 (5)	196 (2)	70
C61	148 (2)	−723 (5)	513 (2)	77
C62	433 (2)	−292 (6)	422 (3)	100
O3	0	311 (5)	250	76
		$[(CH_3Hg)_4(Ad\text{-}2H)]NO_3$ (**3a**)		
Hg3	10556 (1)	−1431 (2)	3636 (1)	44
Hg9	10649 (1)	−2673 (2)	5300 (1)	38
Hg61	4498 (1)	786 (2)	990 (1)	54
Hg62	4781 (1)	86 (3)	2898 (1)	60
O11	982 (2)	−487 (3)	597 (1)	58
O12	1003 (3)	−510 (4)	710 (2)	82
O13	1018 (3)	−254 (4)	663 (2)	105
N1	692 (2)	−18 (4)	208 (2)	52
N3	881 (2)	−116 (4)	320 (2)	39
N6	544 (3)	3 (4)	220 (2)	57
N7	709 (2)	−131 (4)	392 (1)	36
N9	895 (2)	−184 (4)	442 (2)	34
N10	999 (3)	−418 (4)	659 (2)	56
C2	794 (4)	−57 (5)	239 (2)	47
C3	1229 (4)	−165 (5)	416 (3)	71
C4	841 (3)	−135 (4)	364 (2)	27
C5	728 (3)	−102 (5)	335 (2)	44
C6	659 (3)	−32 (6)	260 (2)	54
C8	812 (3)	−184 (4)	457 (2)	36
C9	1230 (3)	−352 (5)	612 (2)	60
C61	357 (4)	148 (7)	−26 (3)	91
C62	403 (4)	27 (7)	353 (3)	86

[a] Hg coordinates are ×10^4; all others are ×10^3. U values have units of Å^2.

the Bruker WH-400 (^1H, 400.13 MHz; ^{13}C, 100.62 MHz) spectrometer (Laboratoire Régional de Résonance Magnétique Nucléaire, Université de Montréal) or the Bruker WP-80 (^{13}C, 20.14 MHz) and WH-90 (^1H, 90 MHz) departmental instruments.

Crystallographic Measurements and Structure Resolutions. Accurate cell parameters and intensity data were obtained at room temperature with an Enraf-Nonius CAD4 diffractometer by using graphite-monochromatized radiation. The detailed procedure is described elsewhere.[20] The data were corrected for the Lorentz effect, polarization, and absorption (Gaussian integration, grid 8 × 8 × 8). Specific details are provided in Table I.

The systematic absences on precession films of **2** (hkl, $h + k \neq 2n$; $h0l$, $l \neq 2n$) were consistent with space groups $C2/c$ and Cc. The distribution of the normalized structure factor amplitudes clearly favored the centric group. The structure was solved by the heavy-atom method in space group $C2/c$ and refined on $|F_o|$. Isotropic refinement of all non-hydrogen atoms was carried out by full-matrix least squares. Hydrogen atoms H2 and H8 were fixed at ideal positions (C–H = 0.95 Å, B = 5.0 Å^2). Their parameters were not refined, but the coordinates were recalculated after each cycle of refinement. Methyl hydrogens were neglected. The refinement was terminated by anisotropically refining all non-hydrogen atoms. The general background in the final difference Fourier map was below ±0.7 e/Å^3, with a few peaks reaching ±1.0 e/Å^3 within 1.3 Å from Hg. No apparent disorder or high correlations showed at any stage of the resolution to suggest that the space group could be Cc instead of $C2/c$.

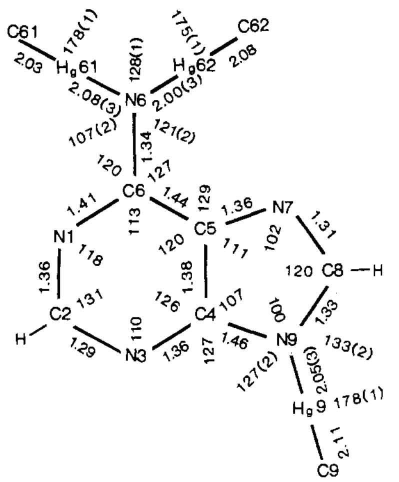

Figure 1. Numbering scheme, interatomic distances (Å), and bond angles (deg) in $[(CH_3Hg)_3(Ad\text{-}2H)]\cdot{}^1/_2H_2O$ (**2**). Unless otherwise stated, esd's are 0.04–0.05 Å on bond lengths and 3° on angles.

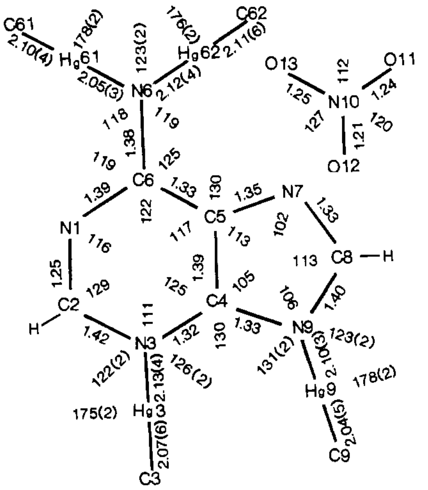

Figure 2. Numbering scheme, interatomic distances (Å), and bond angles (deg) in $[(CH_3Hg)_4(Ad\text{-}2H)]NO_3$ (**3a**). Unless otherwise stated, esd's are 0.04–0.06 Å on bond lengths and 3–4° on angles.

The space group of **3a** was obtained from 25 reflections found by the CAD4 search procedure and centered in the diffractometer counter aperture. Indexation yielded the cell given in Table I, with Niggli parameters unambiguously indicating that no higher symmetry was present. Laue symmetry and cell dimensions were checked with long-exposure Polaroid films taken during oscillation about each axis. Space group $P2_1/c$ was uniquely defined from the systematic absences noted in the full data set ($0k0$, $k \neq 2n$; $h0l$, $l \neq 2n$). The structure was solved by direct methods using the MULTAN package,[21] and the non-hydrogen atoms were anisotropically refined. The hydrogens were treated as described above for **2**. The final difference Fourier map was essentially featureless: general background <±1.5 e/Å^3 and a few peaks of ±(2.2–3.2) e/Å^3 within 1 Å from Hg.

The anomalous dispersion factors of Hg and the scattering curves were from standard sources.[22] The refined coordinates for both compounds are listed in Table II.

Description of the Structures

Compound **2** contains the neutral $[(CH_3Hg)_3(Ad\text{-}2H)]$ molecule schematically represented in Figure 1. Two CH_3Hg^+ groups are bonded to the amino N6 atom, and one extra group is attached to N9. These three sites were those formerly occupied by the adenine protons displaced during the reaction. The Hg–N (av-

---

(20) Bélanger-Gariépy, F.; Beauchamp, A. L. *J. Am. Chem. Soc.* **1980**, *102*, 3461–3464.

(21) Main, P.; Wollfson, M. M.; Lessinger, L.; Germain, G.; Declercq, J. P. "MULTAN, A System of Computer Programs for the Automatic Solution of Crystal Structures from X-ray Diffraction Data", Universities of York, U.K. and Louvain, Belguim, 1978.

(22) Cromer, D. T. *Acta Crystallogr.* **1965**, *18*, 17–23. Cromer, D. T.; Waber, J. T.; *Acta Crystallogr.* **1965**, *18*, 104–109. Stewart, R. F.; Davidson, E. R.; Simpson, W. T. *J. Chem. Phys.* **1965**, *42*, 3175–3187.

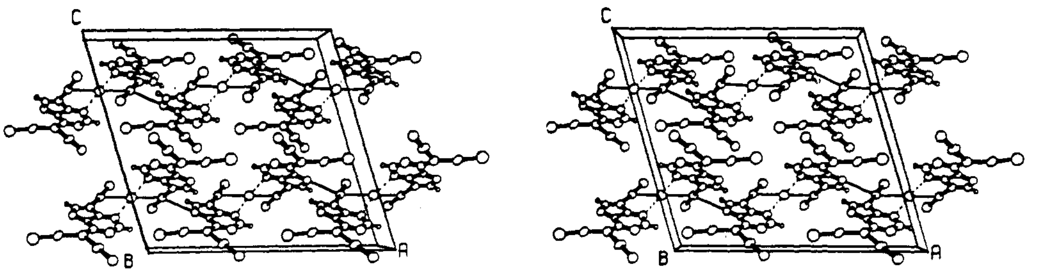

Figure 3. Unit cell of $[(CH_3Hg)_3(Ad\text{-}2H)]\cdot{}^1/_2H_2O$ (**2**) viewed down the *b* axis. Thin bonds and dashed lines represent Hg–O contacts and hydrogen bonds, respectively.

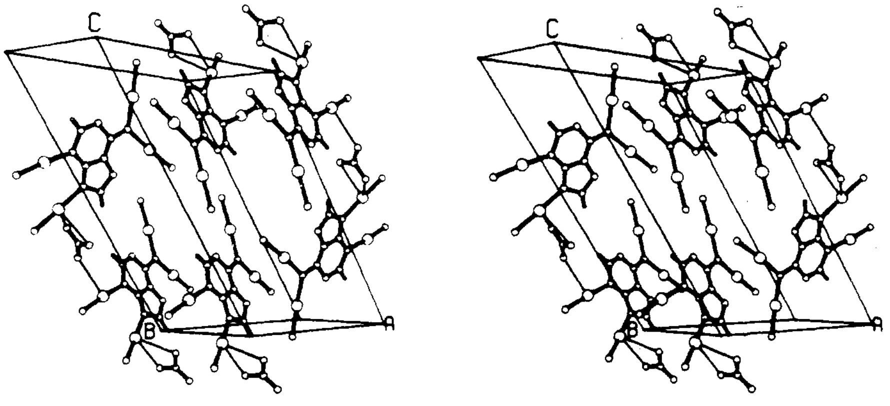

Figure 4. Unit cell of $[(CH_3Hg)_4(Ad\text{-}2H)]NO_3$ (**3a**) viewed down the *ab* diagonal. Thin bonds correspond to Hg–O contacts.

erage 2.04 Å, σ = 0.03 Å) and Hg–C (2.07 Å, σ = 0.04 Å) distances (Figure 1) do not significantly differ from those reported earlier.[1-6] Complex **3a** contains $[(CH_3Hg)_4(Ad\text{-}2H)]^+$ cations (Figure 2), with three CH_3Hg^+ groups occupying the same positions as in **2** and the fourth CH_3Hg^+ group being attached to N3. The Hg–C distances (average 2.08 Å, σ = 0.04–0.06 Å) are similar to those of **2**. The Hg–N bonds (average 2.10 Å, σ = 0.03–0.04 Å) seem to be longer than **2**, but this lengthening is not significant. In both structures, mercury exhibits the usual linear coordination (average H_3C–Hg–N = 177°, σ = 1–2°).

The high esd's preclude any conclusions as to changes in ligand geometry upon complexation. The adenine moiety is best described as two rings, individually planar within 1.5 σ (0.06 Å) and slightly bent about the C4–C5 bond (dihedral angle between five- and six-membered rings = 1.2° for **2**, 2.6° for **3a**). The environment of N6 is also planar within 2.0 σ (0.07 Å). However, the dimercurated amino group as a whole does not lie exactly in the plane of the pyrimidine ring as it ideally should. In complex **2**, only one of the CH_3Hg^+ groups is appreciably displaced from the plane, with a distance of −0.313 (2) Å for Hg62 and −0.84 (4) Å for C62. In **3a**, the $N(HgCH_3)_2$ group is twisted about the C6–N6 bond by 6° and the CH_3Hg^+ groups are found on opposite sides of the pyrimidine plane: Hg61, 0.120 (2) Å; C61, 0.23 (5) Å; Hg62, −0.164 (2) Å; C62, −0.41 (5) Å. These distortions are undoubtedly due to packing forces, which similarly displace to a varying degree the CH_3Hg^+ groups bonded to the endocyclic nitrogens. The atom-to-plane distances (Å) are as follows: in **2**, Hg9, 0.038(1); C9, 0.17 (4); in **3a**, Hg9, 0.073 (1); C9, 0.19 (4); Hg3, −0.237 (2), C3, −0.53 (4). The Hg–Hg separations of 3.66 Å for amino-bonded Hg atoms and 3.41 Å for the Hg3–Hg9 pair are well above the sum of the van der Waals radii (3.0 Å[23]). Distances as short as 3.15 Å have been found for the Hg–Hg contacts in similar structures.[12]

The intramolecular contacts between the amino-bonded Hg atoms and N1 or N7 (Table III) range from 2.79 (3) to 3.06 (3) Å in these two structures. Those on the low side of this range could correspond to some Hg–N bonding interactions. However, the angles are not very favorable. The two C–N–Hg angles at N1 or N7 differ by 69–90°, and they should be equal to correspond to ideal lone pair direction. Similarly, the N6–Hg–N1 and H_3C–Hg–N1 angles, which should be near 90° for optimum interactions, are found to be ~54 and 124°, respectively (Tables VI and XI, supplementary material). Geometry is somewhat more favorable for N7, with N6–Hg–N7 and H_3C–Hg–N7 angles of 72 and 112°, respectively.

Table III. Distances (Å) Involved in Hydrogen Bonds and Contacts with Hg Atoms

	$[(CH_3Hg)_3(Ad\text{-}2H)]\cdot{}^1/_2H_2O$ (**2**)		
Hg9–O3	2.91 (2)	Hg61–N1	2.79 (3)
Hg9–N7[a]	3.10 (3)	Hg62–N7	3.06 (3)
		N3–O3	2.76 (4)
	$[(CH_3Hg)_4(Ad\text{-}2H)]NO_3$ (**3a**)		
Hg3–O11[b]	3.01 (3)	Hg9–O11	2.81 (3)
Hg3–O12[c]	2.95 (3)	Hg9–O11[d]	2.89 (3)
Hg3–O12[b]	2.86 (3)	Hg9–O13	3.13 (4)
Hg3–O13[d]	3.09 (3)	Hg61–N1	2.91 (3)
		Hg62–N7	2.89 (3)

[a] $^1/_2 - x, {}^1/_2 + y, {}^1/_2 - z$. [b] $2 - x, -1 - y, 1 - z$. [c] $x, -{}^1/_2 - y, -{}^1/_2 + z$. [d] $2 - x, -y, 1 - z$.

A view of the unit cell of $[(CH_3Hg)_3(Ad\text{-}2H)]\cdot{}^1/_2H_2O$ is shown in Figure 3. Molecules roughly parallel to the *a* axis, making an angle of ~30° with the *ab* plane, define a V-shaped double ribbon. A water molecule O3 lying on a twofold axis forms hydrogen bonds of 2.76 (3) Å with N3 atoms in two symmetry-related molecules and forms two O···Hg9 contacts of 2.91 (2) Å. Hg9 also forms a long intermolecular contact of 3.10 (3) Å with N7. Cohesion between these ribbons is achieved by stacking interactions between parallel complex molecules.

The structure of **3a** (Figure 4) consists of flat $[(CH_3Hg)_4(Ad\text{-}2H)]^+$ cations stacked roughly parallel to the *ac* plane. The nitrate oxygens form secondary bonds in the range 2.81–2.95 Å with mercury via their O12 and O11 atoms, whereas the shortest Hg–O13 contacts (3.09 Å) correspond to very weak interactions. These NO_3^- ions act as three-way links between complex cations. One of the molecules in the packing diagram shows all the contacts around the Hg3–Hg9 region of a cation. It can be seen that both Hg atoms are completely surrounded in the equatorial plane (assuming the N–Hg–CH_3 direction as axial) by the other Hg atom or nitrate oxygens.

---

(23) Huheey, J. E. *Inorg. Chemistry: Principles of Structure and Reactivity*; Harper & Row: New York, 1972; pp 184–185.

Infrared Spectroscopy

The infrared wavenumbers of compounds **1–3** are compared with those of adenine and CH_3HgAd in Table XVI (supplementary material). The spectra of the corresponding C8-deuteriated compounds are also listed.

CH_3Hg^+ and Anion Vibrations. The CH_3Hg^+ group is detected from various characteristic bands.[6,24,25] A sharp peak is found at 2920 cm^{-1} for the $\nu_s(CH_3)$ mode. The ν_a counterpart, which is usually lost in the strong $\nu(NH_2)$ bands of adenine, is identified as a very weak band at 2980 cm^{-1}. All spectra show a multicomponent absorption at ca. 800 cm^{-1}, including the normally strong $\rho(CH_3)$ vibration. As to the $\delta(CH_3)$ mode expected at 1200 cm^{-1}, it occurs as a shoulder on a strong band originating from ring stretching, but its position could be determined ($\sim$1193 cm^{-1}) with the C8-deuteriated derivatives of $[(CH_3Hg)_2(Ad\text{-}H)]\cdot EtOH$ and $[(CH_3Hg)_3(Ad\text{-}2H)]\cdot{}^1/_2H_2O$, for which the ring mode has shifted. The $\nu(Hg\text{–}C)$ band at $\sim$565 cm^{-1} is visible in all our spectra.

The 1100-cm^{-1} region in the spectrum of $[(CH_3Hg)_4(Ad\text{-}2H)]ClO_4$ is obscured by the very strong ν_3 band of the anion,[26] which also produces the weaker ν_4 absorption at 625 cm^{-1}. A weak shoulder at 925 cm^{-1}, not observed in the corresponding nitrate, is assigned to a normally IR-forbidden ν_1 band, gaining intensity by low-site symmetry. The apparent splitting of the 1100-cm^{-1} band to produce a component at $\sim$1040 cm^{-1} is not due to the anion acting as a monodentate ligand[27] but to a smaller band found at 1040 cm^{-1} in the nitrate, appearing in superposition to the ClO_4^- band here.

In the corresponding nitrate, the strong absorption between 1300 and 1380 cm^{-1} and weaker features at 820 cm^{-1} are due to the NO_3^- ion ν_3 and ν_2 modes, respectively.[26]

N–H Vibrations. Substitution of H9 is accompanied by the disappearance of the broad $\nu(N9\text{–}H)$ absorption centered at 2800 cm^{-1} and of the out-of-plane bending mode at 970 cm^{-1}.[28]

Substitution of the 6-amino group is readily identified. Substitution of both amino protons removes the $\nu(NH_2)$ absorptions in the $[(CH_3Hg)_4(Ad\text{-}2H)]X$ and $[(CH_3Hg)_3(Ad\text{-}2H)]\cdot{}^1/_2H_2O$ spectra. In the monosubstituted $(CH_3Hg)_2(Ad\text{-}H)$ compound, a single $\nu(N6\text{–}H)$ band is found at 3300 cm^{-1}, superimposed on a broad $\nu(O\text{–}H)$ band at $\sim$3170 cm^{-1} due to lattice ethanol. The $\delta(NH_2)$ scissoring mode usually found at 1670 cm^{-1} is absent from all our spectra. The strong and broad $w(NH_2)$ band of adenine at 650 cm^{-1} is removed, leaving only a sharp ring vibration at this position. The very weak absorption at $\sim$620 cm^{-1} for $(CH_3Hg)_3(Ad\text{-}2H)$ and $[(CH_3Hg)_4(Ad\text{-}2H)]NO_3$ is due to another ring mode. A stronger band observed at 615 cm^{-1} for $[(CH_3Hg)_2(Ad\text{-}H)]\cdot{}^1/_2H_2O$ is assigned to $\gamma(N6\text{–}H)$ motion, as a similar strong band was found for the 9-methyladenine (MAd) complex $[Ag_3(MAd\text{-}H)_2]NO_3\cdot 3H_2O$, in which the amino group is also monosubstituted.[29] The $\delta(N6\text{–}H)$ in-plane mode occurs at 1091 cm^{-1}. Some contribution from an ethanol vibration[30] is possible in this region, but this assignment is in good agreement with those proposed for $[(CH_3Hg)_3(Ad\text{-}H)]ClO_4$ (1117 cm^{-1}),[25] $[Ag_3(MAd\text{-}H)_2]NO_3\cdot 3H_2O$ (1123 cm^{-1}),[29] and $[(CH_3Hg)_2(MAd\text{-}H)]NO_3$ (1136 cm^{-1}).[31]

C8-Deuteriation. The normally weak $\nu(C8\text{–}D)$ band is not detected. Two strong absorptions at 945–955 and 590–600 cm^{-1} are directly related to deuteriation at C8. The latter is mainly due to $\gamma(C8\text{–}D)$ motion. The corresponding $\gamma(C8\text{-}H)$ band should occur at $\sim$850 cm^{-1} according to Tsuboi and Kyogoku[32] or at $\sim$910 cm^{-1} according to Lautié and Novak.[28] The latter band is definitely removed by C8-deuteriation. The other band, which shifts to 830 cm^{-1} and loses much intensity in CH_3HgAd,[33] lies in a region where the presence of strong and broad CH_3Hg absorption precludes definitive conclusion.

The new bands at 940 cm^{-1} are mainly due to $\delta(C8\text{-}D)$ motion. The corresponding C8–H motion, coupled with N7–C8 stretching, was calculated to give rise to the 1215-cm^{-1} band of 9-methyladenine.[34] Accordingly, this band disappears from the spectrum of CH_3HgAd by C8-deuteriation.[33] However, the results with the present amino-deprotonated compounds indicate that the above vibration should be discussed in conjunction with the absorption just below 1200 cm^{-1}, involving bending in the C6–N6–H region and stretching of the N1–C2 and N7–C8 bonds.[34] This band, observed at 1156 cm^{-1} in adenine,[28] is shifted to higher wavenumbers by N9-substitution in CH_3HgAd[33] and the present compounds. C8-deuteriation of CH_3HgAd removed the 1235-cm^{-1} band, leaving the strong band at 1193 cm^{-1}. Conversely, the amino-substituted compounds examined here have lost the lower band and retained a strong band at $\sim$1235 cm^{-1}.

Another band involving some $\delta(C8\text{–}H)$ contribution,[34] shifted from 1459 to 1440 cm^{-1} by C8-deuteriation of CH_3HgAd,[33] shows a similar shift for the amino-monosubstituted compound $[(CH_3Hg)_2(Ad\text{-}H)]\cdot EtOH$. However, C8-deuteriation has no effect on this band when both amino protons have been substituted in $(CH_3Hg)_3(Ad\text{-}2H)$ and $[(CH_3Hg)_4(Ad\text{-}2H)]X$.

Ring Vibrations. The shift of the weak imidazole band from 1507 cm^{-1} in adenine to 1485 cm^{-1} was proposed as a characteristic for N9-mercurated N7-free imidazole, since it shifted upward when N7 accepted an extra CH_3Hg^+ ion in higher complexes.[6,25] This generalization is borne out by the constant position of this band at 1485 cm^{-1} in the present compounds, all of which have only one N9-bonded CH_3Hg^+ group on the five-membered ring.

Another interesting feature of all our spectra is the well-defined band at 1120 cm^{-1}, which has been previously observed only for $[(CH_3Hg)_3(Ad\text{-}H)]ClO_4$,[25] a compound in which the amino group is monosubstituted. Therefore, we believe that this band can be used to detect amino mono- or disubstitution by CH_3Hg^+ groups. In an earlier paper,[25] this band was suggested to originate from in-plane N–H bending in the $-NH(HgCH_3)$ group. We now feel that the latter motion occurs at 1092 cm^{-1} in $[(CH_3Hg)_2(Ad\text{-}H)]\cdot EtOH$ and probably at the same position, masked by the ClO_4^- band, in $[(CH_3Hg)_3(Ad\text{-}H)]ClO_4$.[25]

A few vibrations of CH_3HgAd,[33] not markedly affected by amino monosubstitution, are appreciably displaced after disubstitution. The bands at 1596, 1550, and 1460 cm^{-1} undergo shifts of -15 cm^{-1} when the second CH_3Hg^+ substitution takes place on the amino group, whereas the 724-cm^{-1} band, not observed in the spectrum of $(CH_3Hg)_2(Ad\text{-}H)$, occurs at 740 cm^{-1} for the amino-disubstituted compounds. They are not sensitive to whether N3 is free or coordinated.

The influence of N3-substitution shows mainly by the fact that a strong 910-cm^{-1} band observed here for all the N3-free compounds is removed in the 4:1 compounds. Interestingly, this band involves the C8–H portion of the molecule, since it is sensitive to C8-deuteriation. The CH_3HgAd band at 1192 cm^{-1} is shifted to $\sim$1185 cm^{-1} for $[(CH_3Hg)_2(Ad\text{-}H)]\cdot EtOH$ and $[(CH_3Hg)_3(Ad\text{-}2H)]\cdot{}^1/_2H_2O$ and further shifted down to 1173 cm^{-1} for the $[(CH_3Hg)_4(Ad\text{-}2H)]X$ compounds. It is removed by C8 deuteriation.

Nuclear Magnetic Resonance

We recently used multinuclear NMR to investigate the equilibria and exchange processes involving amino-mercurated adenine complexes.[19] The $-N(HgCH_3)_2$ group of the neutral

---

[24] Green, J. H. S. *Spectrochim. Acta, Part A* **1968**, *24A*, 863–884. Butler, I. S.; Newbury, M. L. *Spectrochim. Acta, Part A* **1977**, *33A*, 669–680.

[25] Savoie, R.; Jutier, J. J.; Prizant, L.; Beauchamp, A. L. *Spectrochim. Acta, Part A* **1982**, *38A*, 561–568.

[26] Nakamoto, K. *Infrared Spectra of Inorganic and Coordination Compounds*; Wiley: New York, 1978; pp 142, 244.

[27] Rosenthal, M. R. *J. Chem. Educ.* **1973**, *50*, 331–335.

[28] Lautié, A.; Novak, A. *J. Chim. Phys.* **1974**, *71*, 415–420.

[29] Charland, J. P. Thèse de Doctorat, Université de Montréal, **1984**.

[30] *Aldrich Library of Infrared Spectra*, 3rd ed.; Aldrich: Milwaukee, WI, 1981; No 66B.

[31] Savoie, R.; Poirier, D.; Prizant, L.; Beauchamp, A. L. *J. Raman Spectrosc.* **1981**, *11*, 481–486.

[32] Kyogoku, Y.; Higuchi, S.; Tsuboi, M. *Spectrochim. Acta, Part A* **1967**, *23A*, 969–983.

[33] Charland, J. P.; Beauchamp, A. L. *Croat. Chem. Acta* **1984**, *57*, 679–687.

[34] Tsuboi, M.; Takahashi, S.; Harada, I. *Physico-chemical Properties of Nucleic Acids*; Duchesne, J., Ed.; Academic: New York, 1973; Vol. 2, Chapter 11.

Table IV. ^{13}C NMR Data[a]

		$\delta(^{13}C)$					
	sites	C2	C4	C5	C6	C8	(Hg)CH$_3$
$[(CH_3Hg)_3(Ad\text{-}2H)]$[b] (**1**)	N9, N6, N6	151.06	154.98	123.06	167.27	144.18	2.39
$[(CH_3Hg)_4(Ad\text{-}2H)]NO_3$[c] (**3**)	N9, N6, N6, N3	150.2	149.0	124.4	165.5	144.8	1.7[h]
Δ(**3** − **1**)		−0.9	−6.0	1.3	−1.8	0.6	
anti-$[(CH_3Hg)_2(Ad\text{-}H)]$[b,e] (**2**)	N9, N6	151.70	155.28	120.35	162.43	145.23	0.60
syn-$[(CH_3Hg)_2(Ad\text{-}H)]$[b,e] (**2**)	N9, N6	150.70	155.21	120.81	160.92	145.23	1.20
$[(CH_3Hg)_3(Ad\text{-}H)]NO_3$[c] (**4**)	N9, N6, N3[f]	150.8	151.8	121.3	160.6	147.0	2.3
Δ(**4** − **2**)		−0.4[g]	−3.4	0.7[g]	−1.1[g]	1.8	
$[(CH_3Hg)Dmad]$[c,d] (**5**)	N9	150.3	156.9	120.0	154.30	145.5	0.9
$[(CH_3Hg)_2Dmad]NO_3$[c,d] (**6**)	N9, N3	149.9	151.2	120.7	153.9	146.4	2.0
Δ(**6** − **5**)		−0.4	−5.7	0.7	−0.4	0.9	

[a] In Me$_2$SO-d_6. [b] 100.62 MHz.[19] [c] 20.14 MHz. [d] Reference 35. [e] Slow rotation of the $-NH(HgCH_3)$ group about C6–N6 generates two rotamers, with Hg above N1 (*syn*) or above N7 (*anti*). [f] Major tautomer, see text. [g] Calculated by using mean values for **2**. [h] $^1J(^{199}Hg-^{13}C) = 1560$ Hz.

Table V. ^{1}H NMR Data[a]

		$\delta(^1H)$				
	sites	H2	H8	N6–H	(Hg)CH$_3$	^2J,[g] Hz
$[(CH_3Hg)_3(Ad\text{-}2H)]$[b] (**1**)	N9, N6, N6	7.779	7.562	...	0.653	180
$[(CH_3Hg)_4(Ad\text{-}2H)]NO_3$[c] (**3**)	N9, N6, N6, N3	8.06	7.67	...	0.74	194
Δ(**3** − **1**)		0.28	0.11			
anti-$[(CH_3Hg)_2(Ad\text{-}H)]$[b,e] (**2**)	N9, N6	7.885	7.687	6.20	0.702	190
syn-$[(CH_3Hg)_2(Ad\text{-}H)]$[b,e] (**2**)	N9, N6	7.885	7.687	6.04	0.702	190
$[(CH_3Hg)_3(Ad\text{-}H)]NO_3$[c] (**4**)	N9, N6, N3[f]	8.14	7.89	7.06	0.78	206
Δ(**4** − **2**)		0.26	0.20			
$[(CH_3Hg)Dmad]$[c,d] (**5**)	N9	8.09	7.83	...	0.80	203
$[(CH_3Hg)_2Dmad]NO_3$[c,d] (**6**)	N9, N3	8.39	7.98	...	0.87	218
Δ(**6** − **5**)		0.30	0.15			

[a] In Me$_2$SO-d_6. [b] 400 MHz from ref 19. [c] 80 MHz. [d] Reference 35. [e] See footnote *e* in Table IV. [f] Major tautomer, see text. [g] $^2J(^{199}Hg-^1H)$.

Chart II

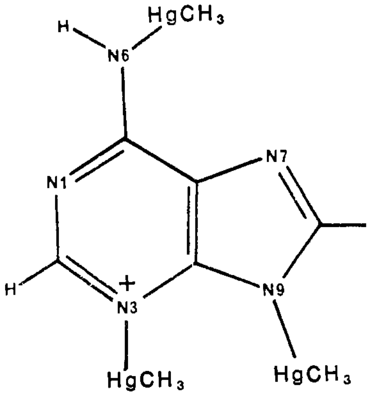

4A

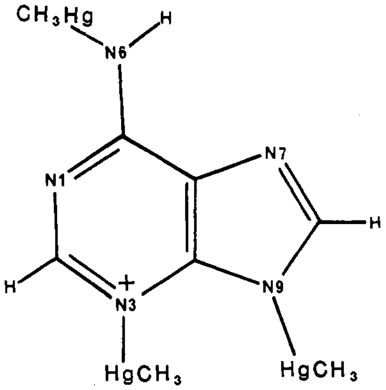

4B

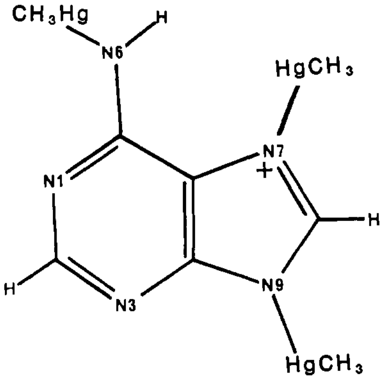

4C

$(CH_3Hg)_3(Ad\text{-}2H)$ molecule (**1**) was shown to be hydrolyzed to some extent by the small amount of water present in Me$_2$SO, producing the $NH(HgCH)_3$-containing species $(CH_3Hg)_2(Ad\text{-}H)$ (**2**):

$$(CH_3Hg)_3(Ad\text{-}2H) + H_2O \rightleftharpoons (CH_3Hg)_2(Ad\text{-}H) + CH_3HgOH \quad (1)$$

The two adenine complexes were in slow exchange at room temperature, and a K_1 value of 0.09 (2) was deduced for reaction 1 from integrations of the H$_2$O and H2 (and H8) signals. The amino-dimercurated $[(CH_3Hg)_4(Ad\text{-}2H)]^+$ cation (**3**) is found here to hydrolyze like **1**. Indeed, besides the major ^{1}H and ^{13}C signals due to **3**, both types of spectra contain a set of minor peaks, which were shown to correspond to the amino-monomercurated species $[(CH_3Hg)_3(Ad\text{-}H)]^+$ (**4**) by comparing with data obtained from a solution of $[(CH_3Hg)_3(Ad\text{-}H)]NO_3$. The K_1 constant for reaction 2, determined as above, is 0.005 (1).

$$[(CH_3Hg)_4(Ad\text{-}2H)]^+ + H_2O \rightleftharpoons [(CH_3Hg)_3(Ad\text{-}H)]^+ + CH_3HgOH \quad (2)$$

The ^{1}H and ^{13}C chemical shift data for the various species are listed in Tables IV and V, respectively. Formation of cation **3** by coordination of CH_3Hg^+ to the N3 lone pair of **1** induces an upfield shift of 6.0 ppm for the C4 signal, the effect being much smaller (0.9 ppm) for the other adjacent C2 carbon. It can reasonably be assumed that the $[(CH_3Hg)_4(Ad\text{-}2H)]^+$ cation (**3**) exists exclusively as the isomer present in the solid (Figure 2), since tautomeric shifts of the N3-bound group to N1 or N7 are opposed by steric hindrance from the bulky $-N(HgCH_3)_2$ substituent at C6. A similar situation is encountered with 6-(dimethylamino)purine (or N^6,N^6-dimethyladenine, HDmad), where access to the N1 or N7 lone pairs is similarly restricted by the bulky $-N(CH_3)_2$ group. Therefore, the N3,N9-coordinated cation identified in the crystals of $[(CH_3Hg)_2(Dmad)]ClO_4$ (**6**)[35] is very probably the only isomer present in solution. By comparing the ^{13}C data for **6** with those of the N9-coordinated $(CH_3Hg)(Dmad)$ molecule (**5**) (Table IV), it is noted that introducing CH_3Hg^+ onto **5** to produce **6** induces upfield shifts similar to those above, that is 5.8 ppm for C4 and 0.4 ppm for C2. Hence, the $[(CH_3Hg)_4(Ad\text{-}2H)]^+$ and $[(CH_3Hg)_2(Dmad)]^+$ cations both exist

---

(35) Grenier, L.; Charland, J. P.; Beauchamp, A. L., manuscript in preparation.

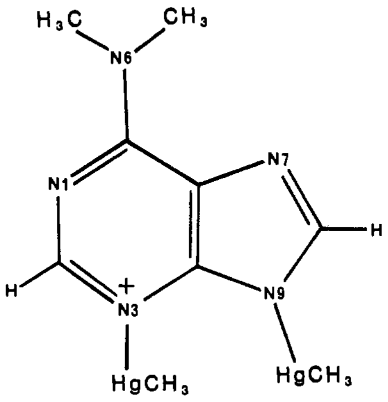

6

in Me_2SO as single isomers, with the cationic CH_3Hg^+ group always bound to N3.

The situation may be different for $[(CH_3Hg)_3(Ad\text{-}H)]^+$ (**4**) (Chart II). The N7 lone pair, which is no longer efficiently shielded, could bind a CH_3Hg^+ group if the $-NH(HgCH_3)$ has the *syn* orientation (Hg above N1) (**4C**). This is the structure suggested by infrared results for cation **4** in solid $[(CH_3Hg)_3(Ad\text{-}H)]X$ ($X = NO_3, ClO_4$).[6] The analogous species with the cationic CH_3Hg^+ group bound to N1 and an *anti* $-NH(HgCH_3)$ group is unlikely to exist because there are no known adenine complexes with a CH_3Hg^+ group bound to N1. Formation of **4** by coordination to a lone pair of **2** is accompanied by an upfield shift of 3.4 ppm for C4 (Table IV). This identifies the N9,N6,N3-tautomer (**4A** and/or **4b**) as the major species, but the shift is substantially less than for the first two systems (~5.8 ppm). It may indicate that some N9,N7,N6-tautomer (**4C**) also exists as a less abundant component. This assumption could also explain the relatively large 1.8 ppm downfield shift observed for the C8 signal, since coordination of CH_3Hg^+ to the N7 lone pair of guanosine and inosine displaces the C8 signal in this direction.[36] Therefore, the $[(CH_3Hg)_3(Ad\text{-}H)]^+$ cation probably exists as unequal proportions of N9,N7,N6- and N9,N6,N3-tautomers in fast exchange, the latter possibly existing as *syn* (**4B**) and *anti* rotamers (**4A**).

The ^1H data for the various compounds are listed in Table V. For the three pairs of compounds discussed above, the $\Delta\delta$ values are found to be greater for H2 than for H8. This is consistent with the cationic CH_3Hg^+ group being bound to the N3 lone pair in all three cationic species. Also noteworthy is the fact that it is for the **4/2** pair that the $\Delta\delta(H8)/\Delta\delta(H2)$ ratio is greatest, which supports the presence of some N7-coordinated tautomer **4C** in solution.

Conclusion

Besides the N9-coordinated CH_3Hg^+ group present in all the adenine complexes reported so far, the compounds studied here have at least one of the amino protons substituted by a CH_3Hg^+ group. This reaction takes place smoothly in water–ethanol mixtures under stoichiometric conditions. The substituted N6 atom retains its sp^2 hybridization, making the resulting $-NH(HgCH_3)$ or $-N(HgCH_3)_2$ units coplanar with the adenine ring. It is not clear whether the intramolecular Hg–N1 and Hg–N7 contacts introduce significant stabilization. What is clear, however, is the steric effect of these substituted amino groups with respect to further coordination to be nearby endocyclic nitrogens. Earlier work on a 9-methyladenine complex has shown that when a monosubstituted $-NH(HgCH_3)$ group is present, an extra CH_3Hg^+ ion can coordinate to N1, while the N6-bonded atom is above N7.[1] The isomeric form with one CH_3Hg^+ group bonded to N7 and the N6-bonded mercury rotated above N1 has not been observed by X-ray diffraction, but on the basis of the ^1H and ^{13}C results, it is likely to exist as a minor tautomeric form of the $[(CH_3Hg)_3(Ad\text{-}H)]^+$ cation is Me_2SO. In the major tautomer, however, the cationic CH_3Hg^+ group is bound to N3. The $-N(HgCH_3)_2$ group shields the N1 and N7 sites more efficiently since the fourth CH_3Hg^+ group in $[(CH_3Hg)_4(Ad\text{-}2H)]NO_3$ is bound to N3 in the solid state and there is no evidence for a different isomeric form in Me_2SO.

Acknowledgment. We wish to thank M. J. Olivier for collecting the X-ray data. Financial support from the Natural Science and Engineering Research Council of Canada and the Ministère de l'Éducation du Québec is gratefully acknowledged.

Supplementary Material Available: Tables of refined temperature factors (Tables VI and XI), calculated coordinates of hydrogen atoms (Tables VII and XII), angles between the contacts with Hg (Tables VIII and XIII), and weighted least-squares planes (Tables IX and XIV) for **2** and **3a** and a list of infrared wavenumbers for **1**–**3** (14 pages); tables of structure factors for **2** and **3a** (Tables X and XV) (19 pages). Ordering information is given on any current masthead page.

---

(36) Buncel, E.; Norris, A. R.; Racz, W. J.; Taylor, S. E. *Inorg. Chem.* **1981**, *20*, 98–103.